Authors

Oliver Meseguer-Ruiz, Timothy J. Osborn, Pablo Sarricolea, Philip D. Jones, Jorge Olcina Cantos, Roberto Serrano-Notivoli, Javier Martin-Vide

Title

Definition of a temporal distribution index for high temporal resolution precipitation data over Peninsular Spain and the Balearic Islands: the fractal dimension; and its synoptic implications

Affiliations

Oliver Meseguer-Ruiz
Departamento de Ciencias Históricas y Geográficas, Universidad de Tarapacá
Group of Climatology, University of Barcelona
2222, 18 de septiembre, Arica, Chile
omeseguer@academicos.uta.cl
+56 5 8220 5255

Timothy J. Osborn
Climatic Research Unit, School of Environmental Sciences, University of East Anglia

Pablo Sarricolea
Department of Geography, University of Chile

Philip D. Jones
Climatic Research Unit, School of Environmental Sciences, University of East Anglia
Center of Excellence for Climate Change Research, Department of Meteorology, King Abdulaziz University, Jeddah, 21589, Saudi Arabia

Jorge Olcina Cantos
Interuniversitary Institute of Geography, University of Alicante

Roberto Serrano-Notivoli
Barcelona Supercomputing Center

Javier Martin-Vide
Climatology Group, Faculty of Geography and History, University of Barcelona

Abstract

Precipitation on the Spanish mainland and in the Balearic archipelago exhibits a high degree of spatial and temporal variability, regardless of the temporal resolution of the data considered. The fractal dimension indicates the property of self-similarity, and in the case of this study, wherein it is applied to the temporal behaviour of rainfall at a fine (10-minute) resolution from a total of 48 observatories, it provides insights into its more or less convective nature. The methodology of Jenkinson and Collison which automatically classifies synoptic situations at the surface, as well as an adaptation of this methodology at 500 hPa, was applied in order to gain insights into the synoptic implications of extreme values of the fractal dimension. The highest fractal dimension values in the study area were observed in places with precipitation that has a more random behaviour over time with generally high totals. Four different regions in which the atmospheric mechanisms giving rise to precipitation at the surface differ from the corresponding above-ground mechanisms have been identified in the study area based on the fractal dimension. In the north of the Iberian Peninsula, high fractal dimension values are linked to a lower frequency of anticyclonic situations, whereas the opposite occurs in the central

region. In the Mediterranean, higher fractal dimension values are associated with a higher frequency of the anticyclonic type and a lower frequency of the advective type from the east. In the south, lower fractal dimension values occur with more frequent anticyclonic–easterly hybrid weather types and with less frequent cyclonic type.

1. The Temporal Fractality of Precipitation

The analysis of temporal variability with respect to climatic components in general is one of the issues which receives much attention in contemporary climatic studies; specifically, precipitation appears as a principal focus of studies in the Iberian Peninsula (Casanueva et al. 2014; De Luis et al. 2010; Gonzalez-Hidalgo et al. 2009; Goodess and Jones 2002; Martin-Vide and Lopez-Bustins 2006; Ramos et al. 2016; Rodríguez-Puebla and Nieto 2010; Rodríguez-Solà et al. 2016; Sáenz et al. 2001, among others). This interest originates from the exigent need to distinguish between natural climatic variability and anthropogenically-induced phenomena. We can speak of climate change not only in terms of a statistically significant increase or decrease in the average of a climate-related parameter, but also whether there is a significant change in variability.

The influence of the Mediterranean Sea is a vital factor in atmospheric processes affecting the Iberian Peninsula, as it plays a major role by introducing peculiarities to the study area. Due to its location and size, the Mediterranean is very sensitive and responds quickly to atmospheric forcing (Lionello 2012). In addition, its western region, which includes the Iberian Peninsula, is affected by a marked inter-annual variability in precipitation, wherein wet years alternate with very dry years (Vicente-Serrano et al. 2011; Trigo et al. 2013), which gives the study area a distinct climatic personality. Despite the trends in recent decades, which indicate that the southeastern area of this region is heading toward a more arid climate (Del Río et al. 2010; González-Hidalgo et al. 2003), it is not free from extreme events with precipitation of a high hourly intensity which has serious consequences at the socio-economic level (Liberato 2014; Trigo et al. 2015). Moreover, Iberia's geography with the Mediterranean to the east means that Southeast Spain gets more rain with easterly winds (Martín-Vide 2004).

As in the case of fractal objects, processes and systems that remain invariant with a change of scale are not defined by any particular scale. A fractal process is one in which the same basic process takes place at different levels; these levels, in turn, reproduce the entire process (Mandelbrot, 1977). The application of these principles has facilitated the description of complex objects and processes which are already widely used and accepted in many fields of the natural sciences including geography, ecology, and new technologies applied to regional information (Goodchild 1980; Goodchild and Mark 1987; Hastings and Sugihara 1994; Peitgen et al. 1992;. Tuček et al. 2011). Due to the fractal behaviour of some atmospheric variables (temperature, precipitation, and atmospheric pressure), fractal analysis has been used in climatic studies to determine the persistence of these variables and their interdependencies (Nunes et al. 2013; Rehman 2009).

Other indicators can be used to define dynamical systems. The Lyapunov exponent (Wolf et al 1985; Wolf 2014) indicates chaos when large and positive, but this application is difficult, even impossible for experimental data records. (Sprott 2003). The fractal dimension can also directly be determined considering the Hurst exponent applied to self-affine series, and is a measure of a data series randomness (Amaro et al. 2004; Malinverno 1990). More recently, other studies have been developed around atmospheric flows that consider the well-known large-scale patterns (ENSO, PDO, NAO…) combined with the chaotic dynamics: the local dimension (Faranda et al. 2017). According to these papers, it seems that these local dimensions are able to represent specific circulation patterns related to time series extreme events.

For some years, these principles have been applied to the spatial distribution of precipitation, rather than its temporal distribution based on an intuitive assumption that a precipitation field may take the form of a fractal object, as it complies with the criterion of self-similarity (Lovejoy and Mandelbrot 1985). When referring to the temporal fractality of precipitation, the concept becomes more abstract; scaling is applied to the duration of the interval for which the occurrence or absence of recorded precipitation is verified, and the same process is repeated at intervals of shorter and longer duration. The purpose of this is to ascertain whether the property of self-similarity is maintained when considering different temporal resolutions.

Several applications have been developed in various disciplines, such as hydrology, from the fractal properties of the spatial and temporal distribution of precipitation (Zhou 2004; Khan and Siddiqui 2012). These fractal processes have been identified in a study on the Spanish mainland from series of accumulated precipitation spanning 90 years, and its analysis demonstrates that its distribution is consistent with a fractal distribution (Oñate Rubalcaba 1997). The values obtained, with an average fractal dimension of 1.32 for the whole territory, are in the same order of magnitude as the fractal dimensions obtained from other macrometeorological and palaeoclimatic records. Fractal analysis also facilitates the identification of trends based on the Mann-Kendall test. One example is the study conducted in the province of La Pampa (Argentina), where this analysis defines trends in more detail than the projections reported by the IPCC-AR4 (Perez et al. 2009). In Venezuela, it has been possible to predict climate changes at different temporal scales based on the same fractal methodology (Amaro et al. 2004). Fractal analysis was also used in studies that have evaluated precipitation trends in regions

169 of the world where access to water is becoming increasingly scarce in parallel with exponential economic
170 growth in recent years (Rehman and Siddiqui 2009; Gao and Hou 2012).
171 The application of this analytical method to regions with precipitation of very high hourly intensity has
172 highlighted several challendes. In these cases, extreme precipitation events conform to models which are even
173 more complex than multi-fractal models, and which depend not only on the occurrence of the phenomenon, but
174 also on the recorded precipitation amounts, which are affected by quantities with very long return periods
175 occurring over very short durations (Dunkerley 2008; García-Marín et al. 2008; Langousis et al. 2009;
176 Veneziano et al. 2006). The importance of the temporal resolution of existing data is particularly apparent in
177 the fractal analysis, as the availability of both hourly and daily data results in significant changes in the values
178 of both the increasing and decreasing fractal dimensions (García Marín 2007; Lopez Lambraño 2014). Another
179 application is the regionalisation of a territory based on a fractal analysis of the temporal distribution of
180 precipitation (Dunkerley 2010; Reiser and Kutiel 2010; Kutiel and Trigo 2014). These studies usually lack
181 references to the mechanisms generating the rainfall under consideration, but it has been found that their results
182 are directly linked to local and regional characteristics, particularly the synoptic origins of precipitation that
183 influences its fractal dimension (Rodriguez et al. 2013; Meseguer-Ruiz and Martín-Vide 2014). It has also been
184 possible to determine, with satisfactory results, the relationship of the fractal dimension with other indices of
185 temporal variability in precipitation, whose significance is well known (coefficient of variation, concentration
186 index, etc.), again as a function of the temporal resolution of the baseline data (Meseguer-Ruiz et al. 2017b).
187 Ghanmi et al. (2013) performed a study in the eastern Mediterranean based on precipitation series with high
188 temporal resolution and have identified three types of temporal structures from Hurst's analysis. The temporal
189 fractality of precipitation in another nearby area, Veneto (Italy), was compared with that of precipitation in the
190 Ecuadorian Amazon province of Pastaza (Kalauzi et al. 2009), and it was concluded that the temporal behaviour
191 of the precipitation events of the two regions are opposite, with decreasing trends in the former case, and
192 increasing trends in the latter. In the western Mediterranean, on the Iberian Peninsula, the highest fractal
193 dimension values have been obtained in areas with higher mean precipitation (Meseguer-Ruiz et al. 2017a).
194 Fractal analysis has also been applied in a very different climatic environment, in India, demonstrating the effect
195 of the monsoon on fractal dimension values (Selvi and Selvaraj 2011). In Queensland, Australia, Breslin and
196 Belward (1999) calculated the fractal dimension of monthly series of precipitation using a methodology based
197 on models for the prediction of cumulative quantities.
198 The aim of this study is to give a synoptic significance to this new indicator of temporal variability in
199 precipitation, which is the fractal dimension, by determining what types of situations at the surface and in the
200 mid-troposphere (500 hPa) are associated with certain values of the Fractal Dimension (FD).
201
202
203 2. Data and Methodology
204 The study was carried out using precipitation data at a temporal resolution of 10 minutes from the databases of
205 48 observatories in the Spanish Meteorological Agency's (AEMET) network of automatic stations (Figure 1).
206 There were initially a total of 75 observatories, but series with missing values of more than 15% were discarded.
207 Values appearing as outliers, i.e. those that exceed physical expectation for rainfall of ten minute duration (here
208 assumed to be those higher than 1.5 times the third quartile) were also eliminated in order to maintain the
209 homogeneity of the series to the greatest extent possible. The total number of values eliminated this way has no
210 significant effects on the results (less than 0.5% of the whole data). Due to the high temporal resolution of the
211 series, we did not attempt to fill missing values.
212 Moreover, a common period was selected for observatories whose series offer guaranteed quality and
213 homogeneity, based on the manual elimination of those records that are out of range, this being the period
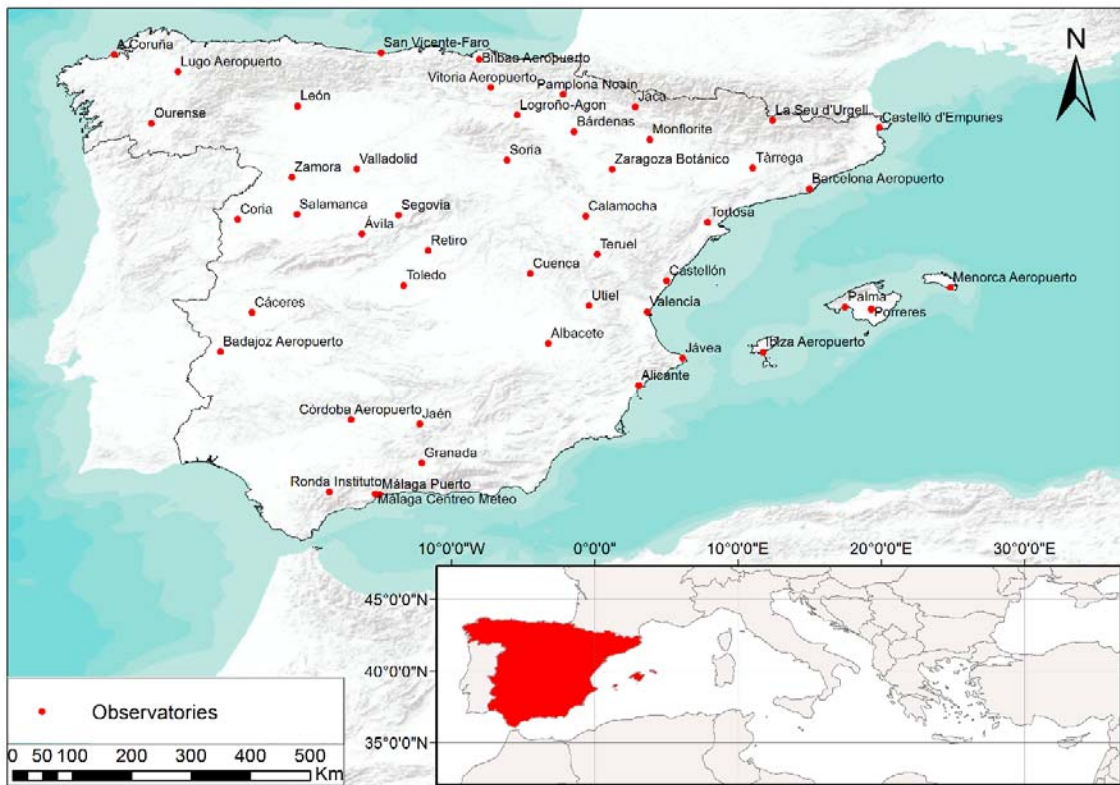214 between 1995 and 2010.
215

Fig. 1. Location of the observatories used in the study

The calculation of the fractal dimension (FD) was performed according to the box-counting method in the following manner: rainfall records with a 10-minute resolution were used, as the 10-minute period is the unit interval which served as the basis for performing the analysis. Then, periods containing 1, 2, 3, 6, 12, 18, 24, 36, 48, 72, 144 and 288 unit intervals, i.e. periods of 10, 20 and 30 minutes, 1, 2, 3, 4, 6, 8, 12, 24 and 48 hours, respectively, were established and the number of those which had greater than zero precipitation was tallied and recorded. The utilisation of 10-minute intervals for two days reflects the intention of studying the occurrence or absence of precipitation on small time scales. The fractal dimension value of the temporal distribution of precipitation is defined on the basis of the slope of the regression line fit to the natural logarithms of l, length of the period in hours, and N, number of periods with greater than zero precipitation. The natural logarithms of these pairs of values for each observatory follow a linear relationship remarkably well. The fractal dimension FD is given by $1+\alpha$, where α is the absolute value of the slope of the regression line (Figure 2). The regression lines for obtaining the FD values at the Ibiza and Lugo observatories are presented by way of illustration.
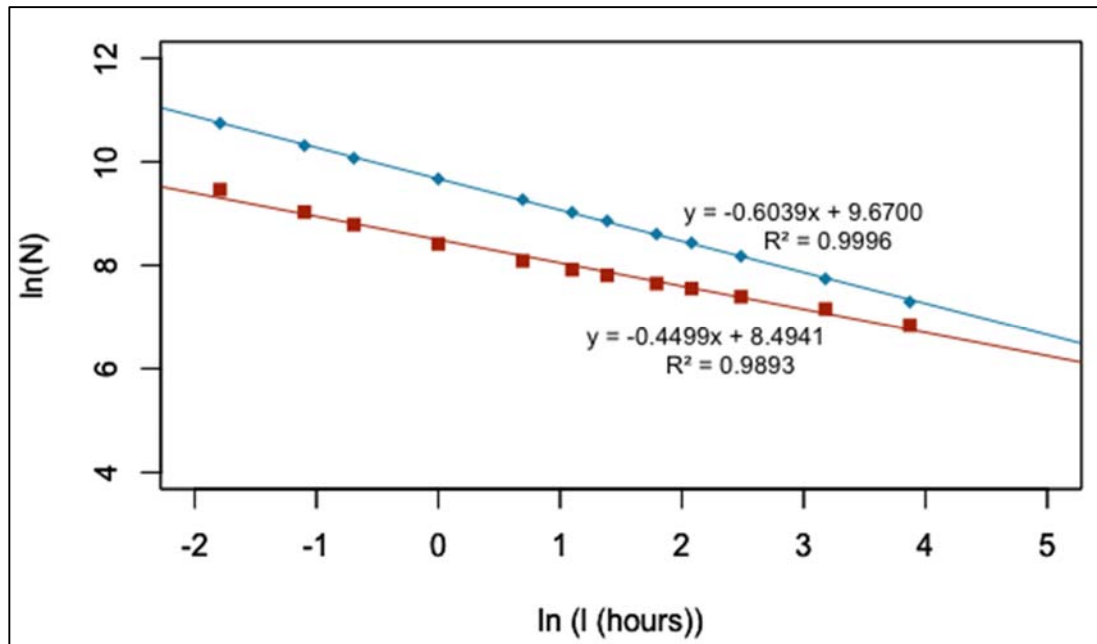
5

232
233 Fig. 2. Regression lines for obtaining FD values in Ibiza (red) and Lugo (blue) during the period from 1997 to
234 2010

235
236 To ensure that the FD results were correct and within proper confidence intervals, a goodness-of-fit analysis
237 was applied by generating several realizations of surrogate data of the same length as the original series. For
238 each station, we simulated 100*n (where n is the station record length in years) series of N with the same mean
239 and standard deviation as the observed data for each l-interval and following a Gaussian process. For instance,
240 for a station with $n = 17$ years of original data, we generated 100*17 values of N in each l-interval, producing
241 1700 simulated annual series with the same structure as the original ones. The FD values were computed for
242 each of these surrogate series and then compared with the original FD value through the calculation of Mean
243 Error (ME), Mean Absolute Error (MAE) and the Root Mean Squared Error (RMSE).
244 Next, a cluster analysis of the 48 observatories was carried out to differentiate the observatories into four groups
245 as a function of latitude, longitude and FD value. A representative observatory with the fewest missing values
246 was selected from each of these groups. The decision on choosing four groups is based on the conclusions
247 obtained in a previous study, where four regions were identified according to a subjective criteria (Meseguer-
248 Ruiz et al. 2017a).
249 As this grouping could mainly depend on the geographical location of the stations and less on the FD values,
250 the cluster analysis was reapplied 1000 times by randomly rearranging the FD corresponding to each location
251 and keeping the latitude and longitude. The resulting cluster assignments were compared with the original by
252 summarizing the coincidences of the groups by station and by clusters.
253 The synoptic classification of Jenkinson and Collison (J&C) (1977) is an automated method which facilitates
254 the determination of the type of atmospheric circulation from atmospheric pressure reduced to sea level at 16
255 points (Figure 3). It is based on the classification of Lamb (1972) and his LWT (Lamb Weather Types) and also
256 proposes J&C weather types (J&CWT) which were developed by Jones et al. (1993).
257 In recent years, there have been several studies which have applied the J&C methodology to various study areas,
258 including the Iberian Peninsula (Grimalt et al. 2013; Martin-Vide 2002; Spellman 2000; Trigo and DaCamara,
259 2000); however, it is not the only synoptic classification that has been applied in this region, as demonstrated
260 by the completion of the COST 733 action for the European continent (Philipp et al. 2014) and various regions
261 of the world outside of the inter-tropical and polar areas, as is the case for Scandinavia, Central Europe, Russia,
262 the United States and Chile (Esteban et al. 2006; Linderson 2001; Pepin et al. 2011; Post et al. 2002; Sarricolea
263 et al. 2014; Soriano et al. 2006; Spellman 2016; Tang et al. 2009).
264 The J&C classification has frequently been used to synoptically characterise variations in different climatic
265 variables with temperature, precipitation and wind being the most studied (Goodess and Jones, 2002; Osborn

266 et al. 1999), but it is also used in climatic modelling for analysing the pressure fields and the simulated
267 deposition of mineral dust (Demuzere and Werner, 2006).
268 Previous work to relate precipitation with specific synoptic situations has successfully demonstrated, for
269 example, the conditions under which a greater amount of precipitation accumulates, or the situations in which
270 more persistent rainfall conditions appear (Martín-Vide et al. 2008). However, synoptic climatology at a high
271 temporal resolution (4 times per day, every 6 hours) has not yet been correlated with indicators of the temporal
272 regularity or irregularity of precipitation in the Iberian Peninsula in order to identify climatic and geographical
273 coherence of the temporal behaviour of precipitation, as has been done in the United Kingdom (Osborn and
274 Jones 2000).
275 A 16-point grid (Figure 3) was chosen in order to enable a better assessment of the Mediterranean and Atlantic
276 influences on the synoptic types which affect the study area. The atmospheric pressure data for this study were
277 obtained for the 1995-2010 ERA Interim (Dee et al. 2011) project, at a resolution of 6 hours at 00:00, 06:00,
278 12:00 and 18:00 UTC. This reanalysis database was selected because it offers a better correlation with the
279 classification of weather types than other products (Jones et al. 2013).
280 The J&C classification consists of 27 weather types: 8 purely advective (N, NE, E, SE, S, SW, W and NW), 1
281 cyclonic (C), 1 anticyclonic (A), 8 advective-cyclonic hybrids (CN, CNE, CE, CSE, CS, CSW, CW and CNW),
282 8 advective-anticyclonic hybrids (AN, ANE, AE, ASE, AS, ASW, AW and ANW) and 1 indeterminate (U).
283 The variables which need to be calculated for the application of the J&C method are the zonal component of
284 the geostrophic wind (W) (in our case between 35° and 45° N), the meridional component of the geostrophic
285 wind (S) (in our case between 20° W and 10° E), the wind direction (D) in azimuthal degrees, the wind speed
286 in m/s (F), the zonal component of vorticity (Z_w), the meridional component of vorticity (Z_s) and total vorticity
287 (Z).
288
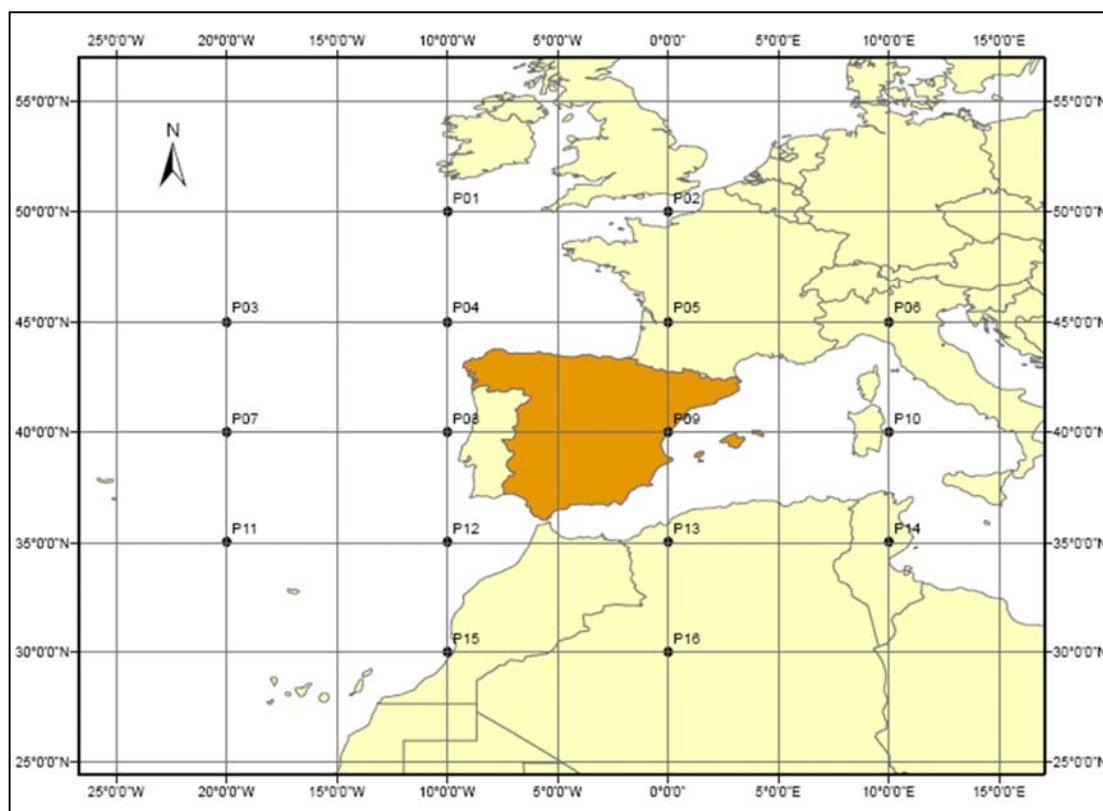
290 Fig. 3. 16-point grid for obtaining the J&C weather types

292 The analytical expressions adjusted for the Iberian Peninsula are as follows:

$$W = 0.5(P12 + P13) - 0.5(P4 + P5)$$

7

$$S = 1.3052[0{,}25(P5 + 2P9 + P13) - 0.25(P4 + 2P8 + P12)]$$

$$F = \sqrt{W^2 + S^2}$$

$$D = \tan^{-1}\left(\frac{W}{S}\right)$$

$$Z_W = 1.1207\left[\frac{1}{2}(P15 + P16) - \frac{1}{2}(P8 + P9)\right] - 0.909\left[\frac{1}{2}(P8 + P9) - \frac{1}{2}(P1 + P2)\right]$$

$$Z_S = 0.852\left[\frac{1}{4}(P6 + 2P10 + P14) - \frac{1}{4}(P5 + 2P9 + P13) - \frac{1}{4}(P4 + 2P8 + P12) + \frac{1}{4}(P3 + 2P7 + P11)\right]$$

$$Z = Z_W + Z_S$$

Based on the values of the above analytical expressions and following the J&C method, the following five rules apply:

- the direction of flow is given by D (8 wind directions are used, accounting for the signs of W and S)
- if $|Z| < F$, there is a purely advective or directional type, defined according to Rule 1 (N, NE, E, SE, S, SW, W and NW)
- if $|Z| > 2F$, there is a cyclonic type (C) if Z> 0, or anticyclonic (A) if Z <0
- if $F < |Z| < 2F$, there is a hybrid type, depending on the sign of Z (Rule 3) and the direction of the flow obtained from Rule 1 (CN, CNE, CE, CSE, CS, CSW, CW, CNW, AN, ANE, AE, ASE, AS, ASW, AW and ANW)
- if F <4.8 and $|Z| <4.2$, there is an indeterminate type (U)

This methodology is used to classify synoptic situations at the sea level and has been adapted to obtain, not a classification of synoptic situations based on two levels (sea level and 500 hPa), but rather an idea of the behaviour of the independent variables (direction and strength of flow, and vorticity) at a higher elevation, in this case, 500 hPa. The methodology used consists in applying the formulae explained above for the calculation of the J&C variables, but using the geopotential elevation at 500 hPa rather than the atmospheric pressure at the surface. In this adaptation, the variables F and Z cannot be expressed in the same units or with the same ranges of magnitude as for the surface analysis, as their calculation is based on geopotential elevations at 500 hPa, but they do reference the above-ground flow behaviour (negative or positive vorticities, moderate or severe intensity of flow, etc.).

For the four observatories selected, the three years which yielded the extreme values of both higher and lower fractal dimensions were chosen. Then, the differences (significant at 95%) between the years in terms of frequency of weather types at the surface and the behaviour of D, F and Z, both at the surface and at 500 hPa were evaluated. In this way, a synoptic significance can be assigned to the concept of fractal dimension based on the location of the observatory.

3. Results

3.1. Grouping based on the Fractal Dimension

The FD values were determined for the 48 selected observatories, corresponding to the slope of the regression line that links the logarithm of the extent of various periods considered (ln (l)) on the x-axis, with the logarithm of the number of those periods in which some precipitation occurred (ln (N)). The FD values for the 48 observatories are shown in Table 1 along with Pearson's R^2 values which, as can be seen, are very high. The FD values range between a maximum of 1.6039 at Lugo Airport and a minimum of 1.4499 at Ibiza Airport, and the R^2 values vary between 0.9998 in Cuenca and 0.9853 at the Barcelona Airport.

Table 1. FD and R^2 values for the 48 observatories in the study

Observatory	FD	R^2	Observatory	FD	R^2
A Coruña	1.5629	0.9994	Málaga CMT	1.5595	0.9959
Albacete	1.4941	0.997	Málaga Puerto	1.5376	0.9943

Alicante	1.4710	0.991	Menorca	1.4680	0.9945
Ávila	1.5000	0.9971	Monflorite	1.5223	0.9906
Badajoz	1.5183	0.9988	Ourense	1.5704	0.9995
Barcelona Aerop.	1.5070	0.9853	Palma	1.4988	0.994
Bárdenas	1.4933	0.9959	Pamplona	1.5487	0.9988
Bilbao	1.5827	0.9997	Porreres	1.4966	0.9952
Cáceres	1.5464	0.9983	Madrid Retiro	1.5432	0.9981
Calamocha	1.4805	0.9946	Ronda	1.5832	0.9982
Castello Empuries	1.5160	0.9968	Salamanca	1.5075	0.9986
Castellón	1.5075	0.9878	San Vicente	1.5839	0.9996
Córdoba	1.5605	0.9983	Segovia	1.5105	0.9976
Coria	1.5644	0.9997	Soria	1.5190	0.9991
Cuenca	1.5468	0.9998	Tàrrega	1.4730	0.9895
Granada	1.5941	0.9981	Teruel	1.4856	0.9909
Ibiza	1.4499	0.9893	Toledo	1.5047	0.9963
Jaca	1.5848	0.9985	Tortosa	1.5160	0.9933
Jaén	1.5573	0.9893	Utiel	1.5058	0.9986
Jávea	1.5101	0.9938	Valencia	1.5258	0.9921
La Seu Urgell	1.5030	0.9953	Valladolid	1.5261	0.9967
León	1.5578	0.9938	Vitoria	1.5559	0.9988
Logroño	1.4961	0.9943	Zamora	1.5020	0.9967
Lugo	1.6039	0.9996	Zaragoza	1.5154	0.9914

These FD were compared with simulated values obtained from the random generation of N values. The goodness-of-fit showed values of MAE, RMSE (Figure 4a) and ME (Figure 4b) near to zero, which means that there were not meaningful differences between observed and simulated. The mean MAE of 0.045, the mean RMSE of 0.056 and the mean ME of -0.0017 between simulated and observed were much lower than the mean difference of ±0.1 between the observed FD values (mean value of 1.5264). Although the differences between observatory FD values is small, it is significant in comparison with the differences between surrogate simulations.
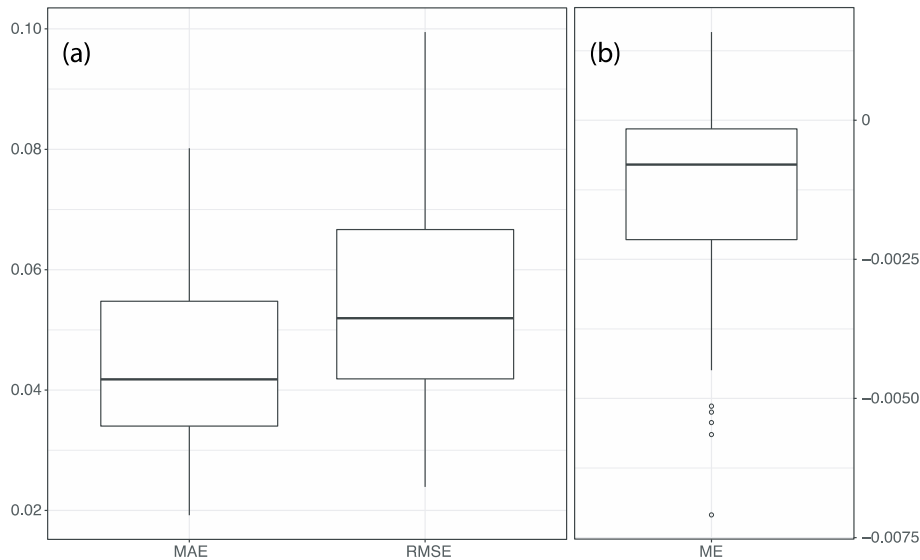

Fig. 4. Statistical estimates of comparison between the original and simulated FD values for the 48 stations. a) Mean Absolute Error (MAE), Root Mean Squared Error (RMSE) and b) Mean Error (ME).

361
362 A cluster analysis that accounts for the latitude and longitude of the observatories was performed based on these
363 values, and the FD values obtained are presented in the above table. This procedure uses a multivariate analysis,
364 namely the cluster analysis, with the aim of differentiating the various observatories into groups with a high
365 degree of external heterogeneity and internal homogeneity. The final centres of the three variables considered
366 for each cluster are listed in Table 3. As can be seen, the differences between the factors considered in each
367 cluster are significant (> 99%), which demonstrates external heterogeneity and internal homogeneity. The
368 groupings are as shown in Table 4 and Figure 5.
369
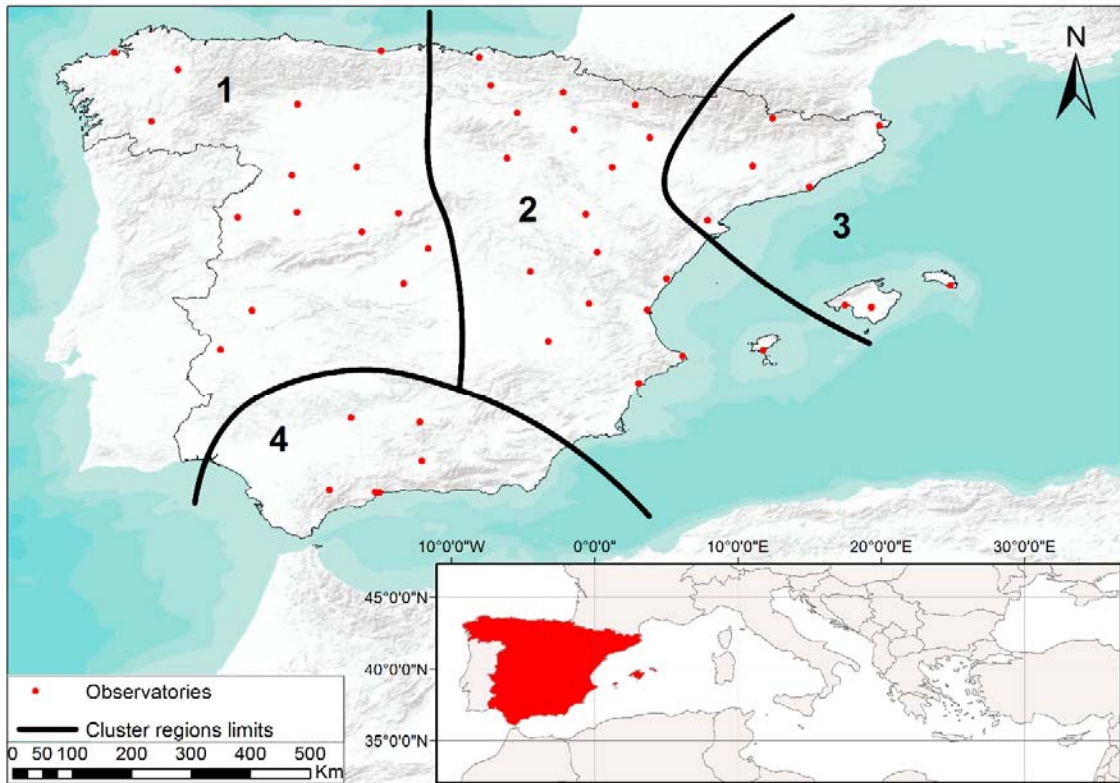
370
371 Fig. 6. Stations grouped together after the cluster analysis
372
373
374 Table 3. Central values for each cluster and significance of the differences

Variable	Cluster 1	Cluster 2	Cluster 3	Cluster 4	p-value
Latitude	41.944	40.506	37.916	41.100	0.000
Longitude	-5.936	1.994	-4.855	-1.533	0.000
FD	1.545	1.494	1.551	1.521	0.001

375
376 Table 4. Groupings of the observatories according to the various clusters

Cluster 1	Cluster 2	Cluster 3	Cluster 4
A Coruña	Albacete	Barcelona Aeropuerto	Córdoba
Ávila	Alicante	Castello Empuries	Granada
Badajoz	Bárdenas	La Seu Urgell	Jaén
Cáceres	Bilbao	Menorca	Málaga CMT
Coria	Calamocha	Palma	Málaga Puerto
León	Castellón	Porreres	Ronda
Lugo	Cuenca	Tàrrega	
Ourense	Ibiza	Tortosa	

Madrid Retiro	Jaca		
Salamanca	Jávea		
San Vicente	Logroño		
Segovia	Monflorite		
Toledo	Pamplona		
Valladolid	Soria		
Zamora	Teruel		
	Utiel		
	Valencia		
	Vitoria		
	Zaragoza		

After the 1000 iterations to compute simulated clusters with randomly rearranged FD values, the comparison with the original groups showed that the clusters are not the same in any simulation. The mean coincidence of each cluster group between the original and the iterated cluster analysis by stations (Figure 6a) was lower than 25%. When we consider the percentage of stations that coincide with their original clusters (Figure 6b), the average of all of them is near to zero, especially in clusters 3 and 4 with only isolated cases with complete coincidence (the number of stations in these original clusters are very much lower than 1 and 2). The iterated cluster analysis showed that the grouping is not only geographic but depends strongly on the FD values. Longitude and latitude have more influence on cluster 1 but not exclusively.
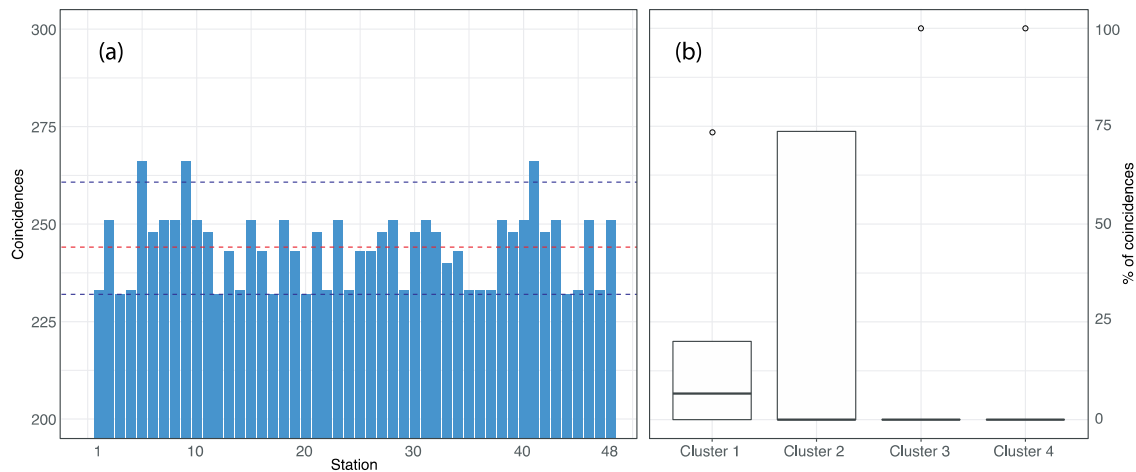
Fig. 6. a) The number of times that a station is placed in the same cluster when using the observed FD values and when using each of the 1000 iterations of randomly rearranged FD values (blue bars). Red dashed line shows the mean number of coincidences and upper and lower dashed blue lines show the 95th and 5th percentile, respectively. b) Boxplot of the percentage of coincident stations by clusters in the same analysis.

The observatories at A Coruña, Castellón, Palma and Jaén were selected as being representative of clusters 1, 2, 3 and 4, respectively, as they are the observatories with the most complete and homogeneous precipitation series in each group. The years and extreme values of FD are shown in Table 5.

Table 5. Years and extreme FD values for the four observatories selected

	A Coruña		Castellón		Palma		Jaén	
	Year	FD	Year	FD	Year	FD	Year	FD
Maximum FD values	2000	1.6160	2002	1.5321	2002	1.5344	1996	1.6065
	2001	1.5957	2004	1.5626	2006	1.5368	2009	1.5987
	2006	1.5968	2006	1.5346	2010	1.5385	2010	1.6385
Minimum FD values	1998	1.5359	1995	1.4190	1995	1.3979	1995	1.4917
	2004	1.5370	1999	1.4649	1999	1.4380	1998	1.4718
	2007	1.4930	2009	1.4380	2005	1.4105	2007	1.5054

398
399 Based on these years, an evaluation was made of the significant synoptic differences appearing both in the types
400 of weather at the surface and in the values of strength, direction and flow vorticity both at the surface and at
401 500 hPa.
402
403 3.2. Types of Weather at the Surface
404 As shown in Table 6, Type A is the most common in the study period (19.23%), followed by Type C (11.27%)
405 and Type E (9.62%). The indeterminate Type U also accounts for a considerable number with 7.16% of the
406 days, as do the purely advective types of the first and fourth quadrants (W, NW, N and NE), with a total of
407 29.47%.
408
409

Table 6. Frequency (%) of the weather types for the reference period 1995-2010

J&C Type	%	J&C Type	%
A	19.23	CS	0.53
AE	2.17	CSE	1.10
AN	1.48	CSW	1.01
ANE	1.54	CW	1.75
ANW	1.45	E	9.62
AS	0.79	N	4.63
ASE	1.24	NE	5.57
ASW	0.99	NW	4.83
AW	1.57	S	1.60
C	11.27	SE	3.88
CE	2.30	SW	3.24
CN	2.09	W	4.83
CNE	2.04	U	7.16
CNW	2.09		

410
411
412 3.3. Synoptic differences at the surface between extreme years for each observatory
413 3.3.1. *A Coruña*
414 At the surface, based on the proportions comparison test, significant differences (> 95%) appear in 10 synoptic
415 types at the A Coruña observatory (Table 7). The highest FD values are associated with years in which
416 anticyclonic situations are less frequent (18.86%) than in years with minimal FD values (20.99%). The hybrid
417 cyclonic types are more frequent from the east (from 1.89% to 3.13%) and from the northeast (1.69% to 2.58%)
418 for years with lower FD. The purely advective types with a SE component (4.47% to 3.17%), SW component
419 (4.15% to 1.80%) and W component (6.09% to 3.63%) are significantly more frequent in the years with
420 maximum FD values, which is the opposite of what occurs with a N component (3.81% to 5.02%) or a NE
421 component (4.93% and 6.84%). Therefore, higher FD values are linked to a higher proportion of SW and W
422 advective situations, while lower FD values are associated with years in which there is a greater proportion of
423 anticyclonic situations.
424
425 Table 7. Cases and percentage of each J&C weather type in years with extreme FD values at the A Coruña
426 observatory

J&C types	Number of cases with highest FD values	%	Number of cases with lowest FD values	%
A	**827**	**18.86**	**920**	**20.99**
AE	88	2.01	90	2.05
AN	69	1.57	68	1.55
ANE	53	1.21	75	1.71
ANW	44	1.00	68	1.55
AS	28	0.64	31	0.71
ASE	68	1.55	56	1.28
ASW	**60**	**1.37**	**25**	**0.57**
AW	**90**	**2.05**	**60**	**1.37**

C	462	10.54	502	11.45
CE	**83**	**1.89**	**137**	**3.13**
CN	81	1.85	86	1.96
CNE	**74**	**1.69**	**113**	**2.58**
CNW	95	2.17	80	1.82
CS	23	0.52	18	0.41
CSE	58	1.32	42	0.96
CSW	47	1.07	23	0.52
CW	84	1.92	68	1.55
E	430	9.81	482	10.99
N	**167**	**3.81**	**220**	**5.02**
NE	**216**	**4.93**	**300**	**6.84**
NW	205	4.68	190	4.33
S	60	1.37	44	1.00
SE	**196**	**4.47**	**139**	**3.17**
SW	**182**	**4.15**	**79**	**1.80**
W	**267**	**6.09**	**159**	**3.63**
U	327	7.46	309	7.05

The bold font indicates statistically significant differences (p<0.05)

For the F variable at the surface, it can be seen from the proportion comparison test that, in years with minimum FD, a significant (> 95%) increase in the frequency of situations between 5 and 7.4 m/s appears; the other categories do not exhibit significant changes. However, at 500 hPa, the changes are significant in more categories; situations with a low flow intensity are more frequent during the years with minimal FD, while in years with maximum FD, situations with average and strong flows appear more frequently (Figure 7).

The direction of flow at the surface exhibits significantly greater prevalence of the first quadrant (NE) in years with minimal FD values, and a higher frequency of flows in the third in years with maximum FD values. The most notable phenomenon above ground is the higher frequency of situations with a SW component in years with maximum FD.

Changes in the vorticity are not very noticeable at the surface; significant differences only appear in the intensities of negative vorticities. However, variations do exist above ground. Slightly negative vorticities are more frequent during years with maximum FD values, and slightly positive vorticities are more frequent during years with minimal FD values.
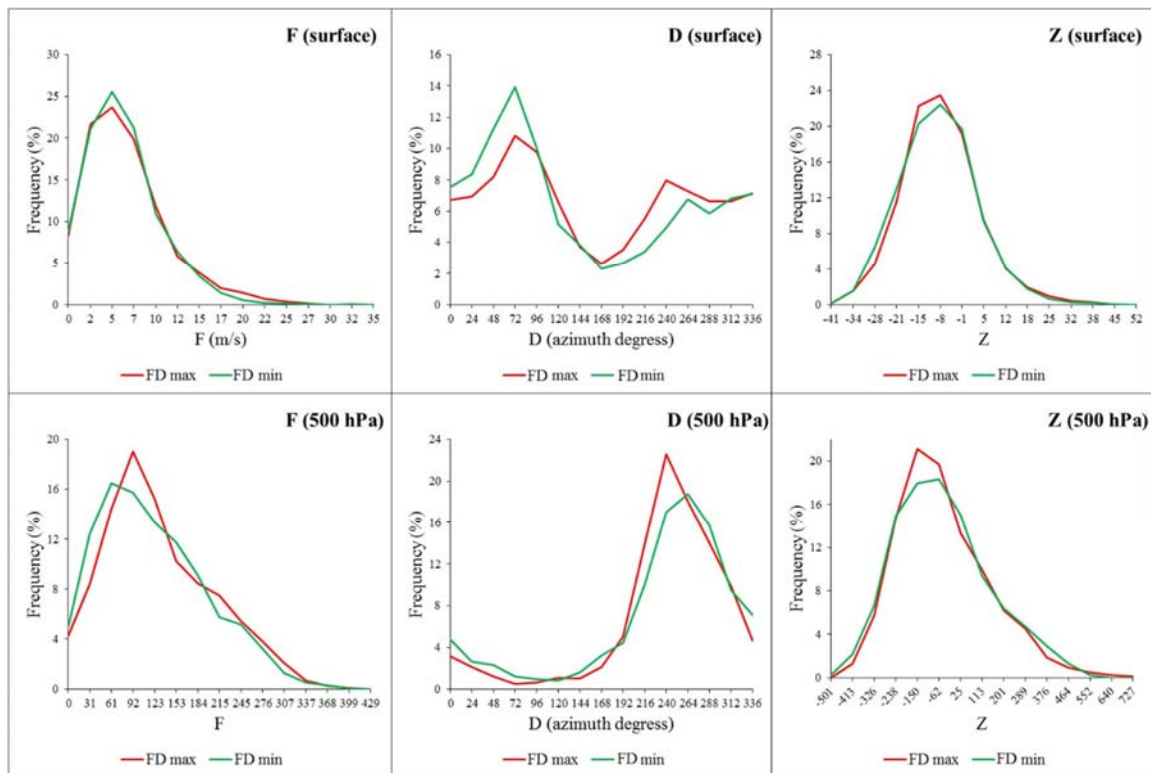
443
444 Fig. 7. Variation of F, D and Z at the surface and at a geopotential height of 500 hPa during years with maximum
445 (red) and minimum (green) values of FD at the A Coruña observatory.
446
447 3.3.2. *Castellón*
448 At the surface, significant differences in the frequency of the synoptic weather types (Table 8) occur, with the
449 purely anticyclonic types begin more recurrent in years with maximum FD values (21.26% vs. 18.11%) and the
450 purely advective types from the east (E) and from the northwest (NW) being more frequent during years with
451 lower FD values (8.67% vs. 11.21% and 4.17% vs. 5.18%, respectively). Significant occurrences of
452 indeterminate Type U are also observed more frequently during years with higher FD values (7.30%) than in
453 years with lower FD values (5.66%).
454
455 Table 8. Cases and percentage of each J&C weather type in years with extreme FD values at the Castellón
456 observatory

J&C types	Number of cases with highest FD values	%	Number of cases with lowest FD values	%
A	**932**	**21.26**	**793**	**18.11**
AE	**74**	**1.69**	**115**	**2.63**
AN	69	1.57	91	2.08
ANE	63	1.44	78	1.78
ANW	64	1.46	82	1.87
AS	**43**	**0.98**	**25**	**0.57**
ASE	**69**	**1.57**	**38**	**0.87**
ASW	46	1.05	57	1.30
AW	**56**	**1.28**	**86**	**1.96**
C	527	12.02	479	10.94
CE	127	2.90	109	2.49
CN	76	1.73	104	2.37
CNE	107	2.44	87	1.99
CNW	79	1.80	90	2.05

CS	17	0.39	18	0.41
CSE	57	1.30	40	0.91
CSW	36	0.82	47	1.07
CW	64	1.46	83	1.89
E	**380**	**8.67**	**491**	**11.21**
N	176	4.01	210	4.79
NE	243	5.54	205	4.68
NW	**183**	**4.17**	**227**	**5.18**
S	63	1.44	47	1.07
SE	146	3.33	156	3.56
SW	148	3.38	142	3.24
W	219	5.00	232	5.30
U	**320**	**7.30**	**248**	**5.66**

The bold font indicates statistically significant differences (p<0.05)

The strength of the flow, represented by the F variable, exhibits significant differences at the surface between the years with maximum FD values during which lower intensities of less than 5 m/s are more frequent, and years with minimal FD values in which moderate F intensities of up to 7.5 m/s are significantly more common. Above ground, in years with higher fractal dimensions, situations with moderate or light winds are most common, while moderately intense wind situations are more normal during years with minimal FD (Figure 8). There are few significant differences in the direction of flow at the surface between the two groupings of years, with situations having north-westerly flow during years with minimal FD values being the only scenario that is more common. Notably, it has been observed that, at 500 hPa, during years with maximum FD values, the flow situation from the south-west is more common than during years with minimal FD.

For its part, the vorticity at the surface exhibits few significant changes. Only situations with markedly negative vorticities occur more frequently during years with maximum FD values. Above ground, however, the situations with more marked negative vorticity are more common during years with minimal FD, whereas neutral vorticities occur more commonly during years with maximum FD.
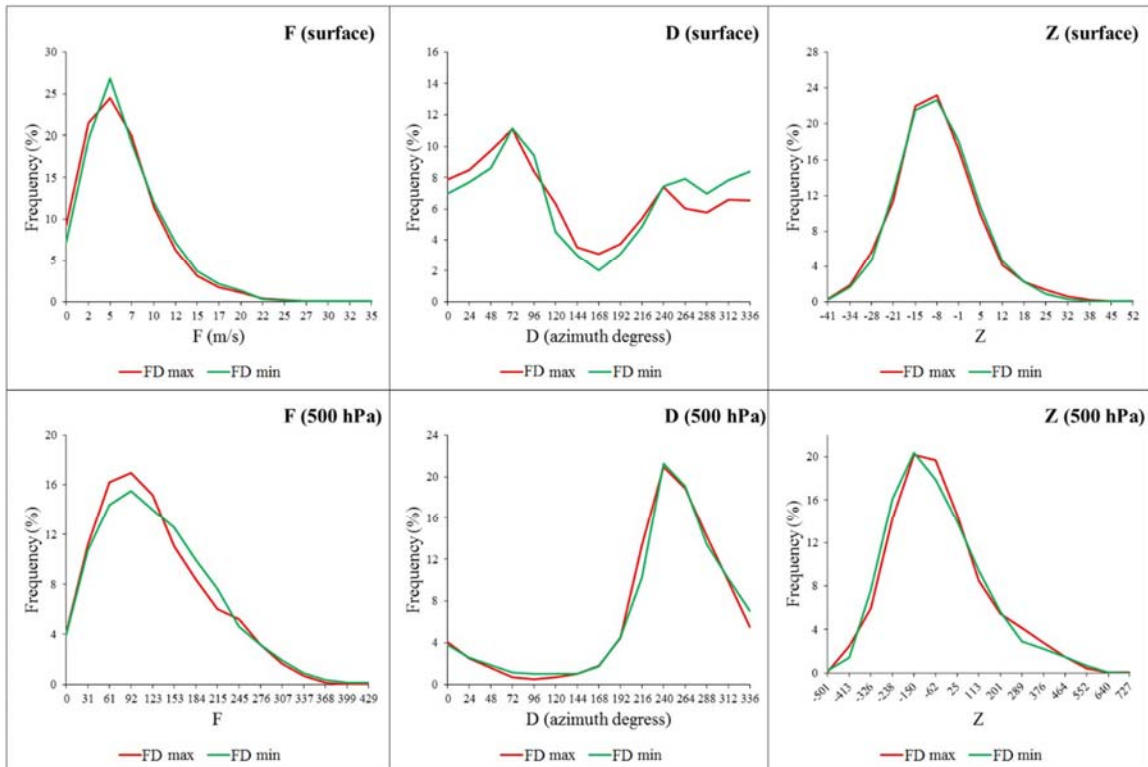
474 Fig. 8. Variation of F, D and Z at the surface and at a geopotential height of 500 hPa during years with maximum
475 (red) and minimum (green) values of FD at the Castellón observatory
476
477 3.3.3. *Palma*
478 The Palma observatory has a higher proportion of anticyclonic days during years with maximum FD values
479 (19.86%) than in years with minimal FD (17.74%). Advective types from the east (E) also experience a
480 substantial significant change, as in the first group of years, these types account for 7.99% of the years, while
481 in the second group, and they account for 11.71%. Advective situations from the south-west also experience
482 significant differences of 4.52% to 3.26% between years with maximum and minimal FD, respectively. Finally,
483 anticyclonic hybrid types with an eastern component (AE, ANE, ASE) also experience significant differences,
484 but these do not exceed 0.76% (Table 9).
485
486 Table 9. Cases and percentage of each J&C weather type in years with extreme FD values at the Palma
487 observatory

J&C types	Number of cases with highest FD values	%	Number of cases with lowest FD values	%
A	**870**	**19.86**	**777**	**17.74**
AE	**91**	**2.08**	**123**	**2.81**
AN	55	1.26	69	1.58
ANE	**47**	**1.07**	**80**	**1.83**
ANW	61	1.39	72	1.64
AS	51	1.16	45	1.03
ASE	**77**	**1.76**	**51**	**1.16**
ASW	52	1.19	46	1.05
AW	55	1.26	71	1.62
C	487	11.12	464	10.59
CE	98	2.24	92	2.10
CN	84	1.92	90	2.05
CNE	100	2.28	92	2.10
CNW	83	1.89	94	2.15
CS	26	0.59	17	0.39
CSE	61	1.39	41	0.94
CSW	39	0.89	39	0.89
CW	66	1.51	63	1.44
E	**350**	**7.99**	**513**	**11.71**
N	193	4.41	227	5.18
NE	265	6.05	264	6.03
NW	187	4.27	203	4.63
S	92	2.10	71	1.62
SE	161	3.68	156	3.56
SW	**198**	**4.52**	**143**	**3.26**
W	220	5.02	211	4.82
U	311	7.10	266	6.07

488 The bold font indicates statistically significant differences (p<0.05)
489
490 The F variable at the surface exhibits significant differences only for moderately strong intensities of above
491 12.35 m/s, and is more common during years with minimal FD values. Above ground, these differences are
492 most noticeable in light-intensity flows which are most common during years with minimal FD, and with flows
493 of medium intensity, while flows with strong intensity occur more frequently in the years with maximum FD
494 values (Figure 9).
495 As for direction, significant changes occur at the surface primarily in the west-south-west component and are
496 more common in years with higher FD values. At 500 hPa, however, greater differences occur. The first-
497 quadrant directions are more common in years with lower FD values, while in the other group of years,
498 situations from the south-west to the north-west are more common.

16

499 At the surface, negative vorticities are more common during years with minimal FD values, while markedly
500 positive vorticities are more common in years with maximum FD values. Above ground, the most significant
501 changes occur with markedly positive vorticities, which are more common during years with maximum FD
502 values.
503
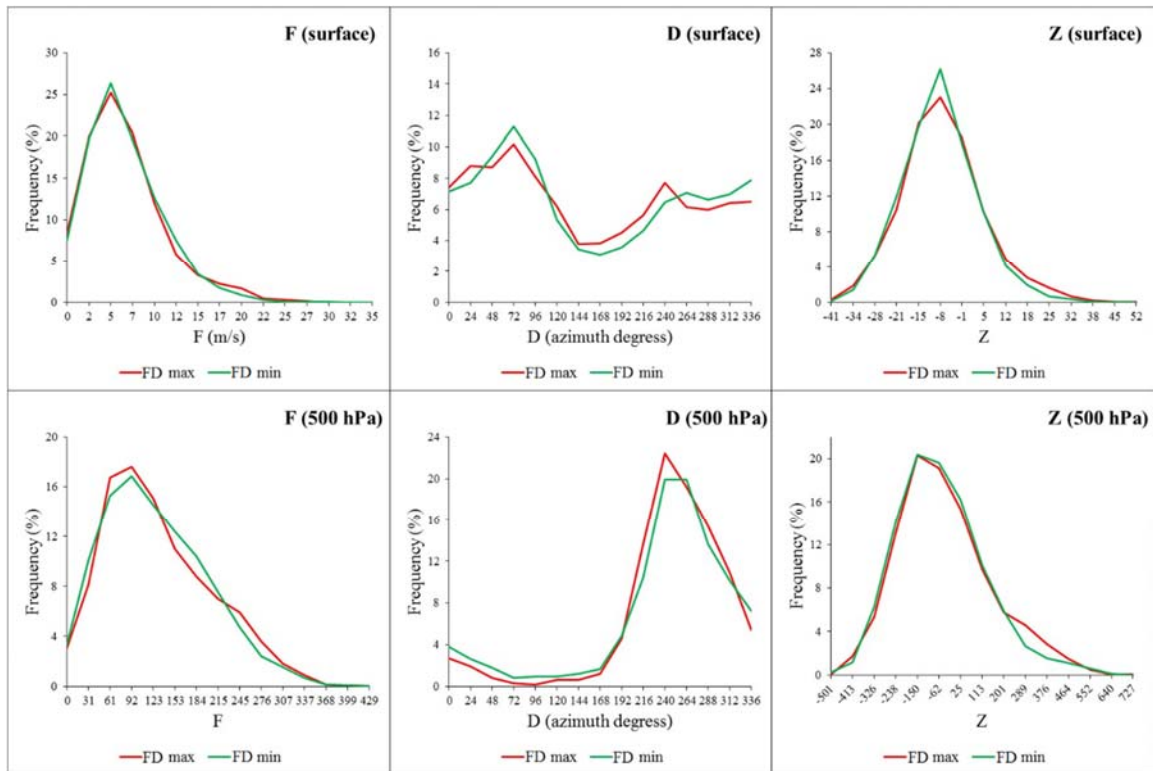
505 Fig. 9. Variation of F, D and Z at the surface and at a geopotential height of 500 hPa during years with maximum
506 (red) and minimum (green) values of FD at the Palma observatory
507

508 3.3.4. *Jaén*
509 At Jaén, the anticyclonic and cyclonic types are the only ones which undergo significant changes. During years
510 with maximum FD values, Type A is less frequent (16.95%), and Type C is more frequent (11.79%) compared
511 with years with lower FD values, in which Type A has increased (19.84%) and C has decreased (9.57%). The
512 N and E purely advective types also increase in the second group (from 9.72% to 11.16%, and 4.49% to 5.71%
513 respectively), while the SW and indeterminate (U) types are less frequent (4.11% to 2.69% and 7.25% to 6.19%)
514 (Table 10).
515

516 Table 10. Cases and percentage of each J&C weather type in years with extreme FD values at the Jaén
517 observatory

J&C types	Number of cases with highest FD values	%	Number of cases with lowest FD values	%
A	**743**	**16.95**	**869**	**19.84**
AE	113	2.58	102	2.33
AN	76	1.73	61	1.39
ANE	61	1.39	72	1.64
ANW	66	1.51	72	1.64
AS	29	0.66	40	0.91
ASE	34	0.78	65	1.48
ASW	61	1.39	31	0.71
AW	56	1.28	83	1.89
C	**517**	**11.79**	**419**	**9.57**

CE	104	2.37	116	2.65
CN	98	2.24	93	2.12
CNE	85	1.94	97	2.21
CNW	86	1.96	84	1.92
CS	33	0.75	23	0.53
CSE	42	0.96	46	1.05
CSW	43	0.98	32	0.73
CW	82	1.87	64	1.46
E	**426**	**9.72**	**489**	**11.16**
N	**197**	**4.49**	**250**	**5.71**
NE	255	5.82	279	6.37
NW	266	6.07	195	4.45
S	67	1.53	66	1.51
SE	157	3.58	162	3.70
SW	**180**	**4.11**	**118**	**2.69**
W	189	4.31	181	4.13
U	**318**	**7.25**	**271**	**6.19**

The bold font indicates statistically significant differences (p<0.05)

The F variable at the surface exhibits moderate intensities significantly more frequently during years with higher FD values, but the more moderate and average flows appear more frequently during years with lower FD values. The higher flow intensities, however, occur in years with maximum FD values. At higher elevations, mild intensities appear more commonly in the second group of years, while, similar to observations at the surface, strong intensities are more common in the first group.

At the surface, the most significant variations occur in situations with an eastern component, which are more common in years with minimal FD, in those with a south-south-western component, which exhibit more frequent significant variations during years with maximum FD values, and those with a westerly component, which again exhibit more common significant variation during years of minimal FD. At 500 hPa, flows with a westerly component are significantly more common during years with maximum FD values, with the exception of flows coming purely from the west which are significantly more common during years with minimal FD values (Figure 10).

As for the vorticity at the surface, it is significant that during years with higher FD values, positive vorticities are more frequent, while negative vorticities are more common during years with minimal FD values. The same pattern is repeated at 500 hPa with the exception of positive vorticities which are more frequent in the second group of years.
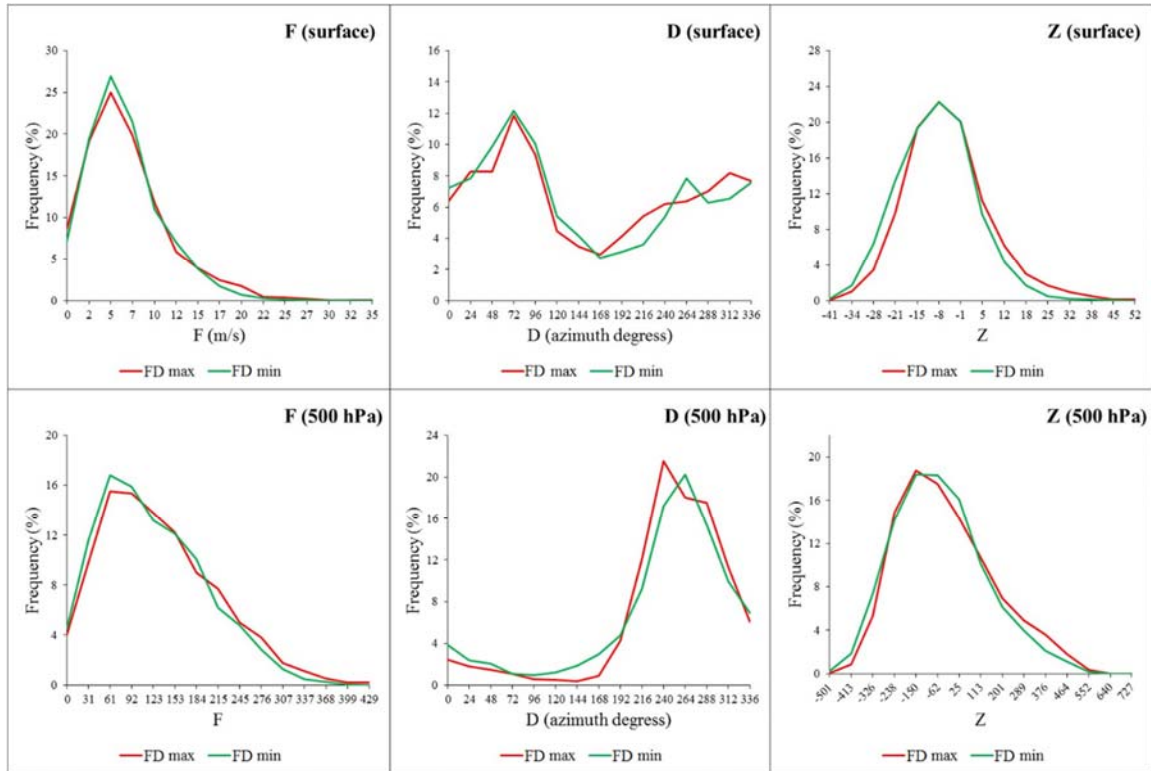
Fig. 10. Variation of F, D and Z at the surface and at a geopotential height of 500 hPa during years with maximum (red) and minimum (green) values of FD at the Jaén observatory

4. Discussion and Conclusions

The fractal dimension values obtained for the 48 observatories in the study range between 1.4499 and 1.6039. These FD values are not comparable with those of other published studies on similar study areas (Meseguer-Ruiz et al. 2014), as the temporal resolutions of the series used are different. The resolution in the above mentioned study was 30 minutes, whereas the temporal resolution for this study is 10 minutes. This usually results in the FD data obtained in other studies being lower, as there are no data entries for intervals of 10 and 20 minutes, so that upon obtaining the corresponding natural logarithms and drawing the regression line, the absolute value of its slope is lower and, therefore, so is the FD value.

Breslin and Belward (1999) propose an alternative method to box-counting and Hurst's R/S analysis for calculating the fractal dimension of a temporal precipitation series based on the variation of monthly precipitation totals. The Breslin and Belward (1999) procedure, which consists of calculating the fractal dimension based on precipitation intervals instead of boxes, enables the calculation of the fractal dimension on a monthly basis, but not at a 10-minute resolution, as many of the values of the series are null and are also closely spaced; therefore, the variation in this type of series would often be null.

The FD values obtained for Tunisia in Ghanmi et al. (2013) are comparable to those of this study, as they were calculated based on precipitation series at a 5-minute resolution following a box-counting method. These values cluster around 1.44, which makes them very similar to those found in areas of the Spanish mainland with less precipitation (Levante, south-eastern Iberian Peninsula and the Ebro valley) and the Balearic Islands (1.4499 in Ibiza), which are regions in which the climate is similar to that of Tunisia, with dry and warm summers and mild, moderately rainy winters. The analysis of the 4 stations shows that few of the hybrids have significant differences. The value obtained in the study of Oñate-Rubalcaba (1997) is notably different with those obtained in this study. This could be explained, first of all, by the different time resolutions considered, annual in the first case, 10-minutes in the present work. Such a difference can also be explained because of the different method used to calculate the fractal dimension, Hurst exponent versus box counting method.

567   In short, it can be concluded that the fractal dimension values in temporal series in the Iberian Peninsula and
568   the Balearic Islands depend on the location and rainfall at the observatory. The highest value was found at the
569   Lugo Airport observatory (1.6039), and the lowest value at Ibiza Airport (1.4499). At lower FD values, the
570   property of self-similarity was fulfilled, to a large extent, in the temporal distribution of precipitation, and
571   conversely, at greater FD values, it was fulfilled to a lesser extent; this finding coincides with the results
572   presented in Selvi et al. (2011). In addition, the link between FD values and precipitation totals has not been
573   studied.

574   The regional differentiation of the Spanish mainland, carried out as a function of FD, coincides with the results
575   of various studies (Rodríguez-Puebla and Nieto 2010; Rodríguez-Solà et al. 2016) which delineate a northern
576   region in which rainfall is associated with the arrival of Atlantic squalls corresponding to cyclonic types, which
577   penetrate the mainland and see a decrease in the rainfall contribution. These situations barely bring precipitation
578   into Mediterranean Spain, where rain is linked to easterly storms or to the settling of squalls in the Gulf of Leon,
579   in the western Mediterranean. In the south, rainfalls are associated with squalls settled in the Alboran Sea or off
580   the coast of Cadiz, and circulate through the Guadalquivir valley, where episodes of rain usually wind down.

581   When comparing the results obtained from the list of J&C weather types with those obtained in other studies in
582   a coincident study area (Spellman 2000; Grimalt et al. 2013), there are significant differences in the frequencies
583   of the weather types which have a higher occurrence throughout the year (A, C, U, NE, E, W). Type A occurs
584   at a frequency of 23.37% in the study of Spellman (2000), at 21% for Grimalt et al. (2013) and at 19.23% in
585   the present study. The frequencies of Type C (14.58%, 19% and 11.27%) are also different, as are those of Type
586   NE (6.73%, 3.1% and 5.57%), those of Type E (4.32%, 2.2% and 9.62%), those of Type W (4.33%, 3.4% and
587   4.83%), and especially those of Type U (18.14%, 27% and 7.16% respectively). The results obtained by Rasilla
588   Alvarez (2003) also differ slightly from those obtained in this study, and as it concerns a hybrid classification
589   (with objective properties from Principal Component Analysis, as well as subjective properties), the results are
590   not comparable. In other areas of the world, the proportions obtained are similar in terms of the prevalence of
591   anticyclonic types (Pepin et al. 2011; Sarricolea et al. 2014), but have little or even no Type U. This is due to
592   the geographical properties of the study area which has a quasi-inland sea to the east, a phenomenon which does
593   not occur in other parts of the world with a Mediterranean climate, and frequently occurring, insignificantly
594   contracted pressure fields during the summer.

595   The differences with respect to the Spellman (2000) study have two principal causes; first, the grid used in the
596   study from 2000 had 9 points as opposed to the 16 that were used in this study, so the area covered is greater
597   and, therefore, provides different pressure gradients. Another explanation, which particularly affects Type U,
598   is that in the first study, a threshold of 6, below which the indeterminate type is defined, was used for the
599   strength and vorticity of flow. Another study (Goodess and Jones, 2002) states that the threshold of 6 is correct
600   for the British Isles as proposed in the original methodology (1977), but for the Iberian Peninsula, it must be
601   reduced to 4.8 and 4.2 for the strength and vorticity, respectively, as the circulation is less vigorous in the latter
602   case. The same is true regarding the work of Grimalt et al. (2013). It may be interesting to choose a finer grid
603   in the future to better cover heavy precipitation events that are much more localized.

604   The grid proposed in this paper is displaced 5° to the east, which results in a higher probability of recording
605   barometric swamp situations than the grid which is presented in the Spellman (2000) study. Moreover, the
606   smaller the space in which the J&C methodology is applied, the more difficult it will be to identify the
607   barometric gradient; therefore, it is common for the frequency of the U type to increase. The 16-point grid also
608   provides a more reliable reflection of the dominant flows in the study area.

609   In view of the results obtained in the application of J&C in the fractal dimensions, and being aware that the
610   sample of years used is not desirable in terms of its length, we can state that the synoptic significance of higher
611   or lower fractal dimension values depends firstly on the region in which the observatory is located and therefore,
612   on the atmospheric mechanisms which give rise to precipitation. To summarize, it could be argued that the
613   higher fractal dimensions in the Atlantic half of the peninsula are associated with weather types in which
614   cyclonic and advective types have prevailed most frequently, as these are the weather types which give rise to
615   rainfall in this part of the study area. The greatest frequency of this type of mechanism implies that precipitation
616   is more frequent and random, and is furthest removed from the property of perfect self-similarity in the temporal
617   distribution of precipitation. In contrast, when anticyclonic types dominate more, precipitation is scarce and,
618   therefore, its occurrence is more sporadic and concentrated, fulfilling self-similarity to a greater extent and
619   yielding lower FD values. However, in the Mediterranean part of the Iberian Peninsula, the high FD values high
620   are associated with a higher frequency of Type A, because if a general anticyclonic situation occurs, the flows
621   from the west and the Atlantic squalls will not affect the Iberian Peninsula. Nevertheless, with that situation in
622   the Mediterranean, flows or local mechanisms that give rise to precipitation may operate in this area (Pionello

623 2012). The years with lower fractal dimension values are associated with flows from the first quadrant, which
624 cause rains in the eastern mainland, but they are not very frequent or recurring throughout the year; therefore
625 the property of self-similarity is less clear. Due to the temporal resolution available for the precipitation data, it
626 is possible that this variable records variations based on the microclimatic properties of the site under
627 consideration. These are processes of low spatial dimension which are not reflected in a grid of the dimensions
628 available for this study, and for which one would have to consider applying poorly developed latitudinal and
629 longitudinal grids.
630
631

632 References
633 Amaro IR, Demey JR, Macchiavelli R (2004) Aplicación del Análisis R/S de Hurst para estudiar las propiedades
634 fractales de la precipitación en Venezuela. Interciencia 29(011): 617-620
635 Breslin MC, Belward JA (1999) Fractal dimensions for rainfall time series. Math Comput Simulat 48: 437-446.
636 doi: 10.1016/S0378-4754(99)00023-3
637 Casanueva A, Rodríguez-Puebla C, Frías MD, González-Reviriego N (2014) Variability of extreme
638 precipitation over Europe and its relationships with teleconnection patterns. Hydrol Earth Syst Sc 18: 709-725.
639 doi: 10.5194/hess-18-709-2014
640 De Luis M, Brunetti M, Gonzalez-Hidalgo JC, Longares LA, Martin-Vide J (2010) Changes in seasonal
641 precipitation in the Iberian Peninsula during 1946-2005. Global Planet Change 74: 27-33. doi:
642 10.1016/j.gloplacha.2010.06.006
643 Del Río S, Herrero L, Fraile R, Penas A (2011) Spatial distribution of recent rainfall trends in Spain (1961-
644 2006). Int J Climatol 31: 656-667. doi: 10.1002/joc.2111
645 Dee DP, Uppala SM, Simmons AJ et al (2011) The ERA-Interim reanalysis: configuration and performance of
646 the data assimilation system. Q J Roy Meteor Soc 137: 553–597. doi: 10.1002/qj.828
647 Demuzere M, Werner M (2006) Jenkinson-Collison classifications as a method for analyzing GCM-scenario
648 pressure fields, with respect to past and future climate change and European simulated mineral dust deposition.
649 Dissertation, Max Planck Institute for Biogeochemistry
650 Dunkerley D. 2008. Rain event properties in nature and in rainfall simulation experiments: a comparative review
651 with recommendations for increasingly systematic study and reporting. Hydrol Process 22: 4415-4435. doi:
652 10.1002/hyp.7045
653 Dunkerley DL (2010) How do the rain rates of sub-events intervals such as the maximum 5- and 15-min rates
654 (I_5 or I_{30}) relate to the properties of the enclosing rainfall event? Hydrol Process 24: 2425-2439. doi:
655 10.1002/hyp.7650
656 Esteban P, Martin-Vide J, Mases M (2006) Daily atmospheric circulation catalogue for Western Europe using
657 multivariate techniques. Int J Climatol 26: 1501-1515. doi: 10.1002/joc.1391
658 Faranda D, Messori G, Yiou P (2017) Dynamical proxies of North Atlantic predictability and extremes. Sci
659 Rep-UK 7: 41278. doi: 10.1038/srep41278
660 Gao M, Hou X (2012) Trends and multifractal analysis of precipitation data from Shandong peninsula, China.
661 American Journal of Environmental Sciences 8(3): 271-279
662 García-Marín AP (2007) Análisis multifractal de series de datos pluviométricos en Andalucía. PhD Thesis,
663 University of Córdoba, Córdoba
664 García-Marín AP, Jiménez-Hornero FJ, Ayuso-Muñoz JL (2008) Universal multifractal description of an hourly
665 rainfall time series from a location in southern Spain. Atmosfera 21(4): 347-355
666 Ghanmi H, Bargaoui Z, Mallet C (2013) Investigation of the fractal dimension of rainfall occurrence in a semi-
667 arid Mediterranean climate. Hydrolog Sci J 58(3): 483-497. doi: 10.1080/02626667.2013.775446
668 González-Hidalgo JC, De Luís M, Raventós J, Sánchez J.R. (2003) Daily rainfall trend in the Valencia Region
669 of Spain. Theor Appl Climatol 75: 117-130. doi: 10.1007/s00704-002-0718-0
670 Gonzalez-Hidalgo JC, Lopez-Bustins JA, Štepánek P, Martin-Vide J, de Luis M (2009) Monthly precipitation
671 trends on the Mediterranean fringe of the Iberian Peninsula during the second half of the twentieth century
672 (1951-2000). Int J Climatol 29: 1415-1429. doi: 10.1002/joc.1780
673 Goodchild MF (1980) Fractals and the accuracy of geographical measures. Math Geol 12(2): 85-98. doi:
674 10.1007/BF01035241
675 Goodchild MF, Mark DM (1987) The Fractal Nature of Geographic Phenomena. Ann Assoc Am Geogr 77(2):
676 265-278. doi: 10.1111/j.1467-8306.1987.tb00158.x
677 Goodess CM, Jones PD (2002) Links between circulation and changes in the characteristics of Iberian rainfall.
678 Int J Climatol 22: 1593-1615. doi: 10.1002/joc.810

679   Grimalt M, Tomàs M, Alomar G, Martín-Vide J, Moreno-García MDC (2013) Determination of the Jenkinson
680   and Collison´s weather types for the western Mediterranean basin over 1948-2009 period. Temporal analysis.
681   Atmosfera 26: 75-94. doi: 10.1016/S0187-6236(13)71063-4

682   Hastings HM, Sugihara G (1994) Fractals: A User's Guide for the Natural Sciences. Oxford University Press,
683   Oxford

684   Jenkinson AF, Collison P (1977) An initial climatology of gales over the North Sea. Synoptic Climatology
685   Branch Memorandum nº 62, Bracknell, Meteorological Office, London

686   Jones PD, Hulme M, Briffa KR (1993) A comparison of Lamb circulation types with an objective classification
687   scheme. Int J Climatol 13: 655-663. doi: 10.1002/joc.3370130606

688   Jones PD, Harpham C, Briffa KR (2013) Lamb weather types derived from reanalysis products. Int J Climatol
689   33: 1129-1139. doi: 10.1002/joc.3498

690   Kalauzi A, Cukic M, Millá H, Bonafoni S, Biondi R (2009) Comparison of fractal dimension oscillations and
691   trends of rainfall data from Pastaza Province, Ecuador and Veneto, Italy. Atmos Res 93: 673-679. doi:
692   10.1016/j.atmosres.2009.02.007

693   Khan MS, Siddiqui TA (2012) Estimation of fractal dimension of a noisy time series. International Journal of
694   Computer Applications 45(10): 1-6

695   Kutiel H, Trigo RM. 2014. The rainfall regime in Lisbon in the last 150 years. Theor Appl Climatol 118: 387-
696   403. doi: 10.1007/s00704-013-1066-y

697   Lamb HH (1972) British Isles weather types and a register of daily sequence of circulation patterns, 1861-1971.
698   Geophysical Memoir 116, HMSO, London

699   Langousis A, Veneziano D, Furcolo P, Lepore C (2009) Multifractal rainfall extremes: Theoretical analysis and
700   practical estimation. Chaos Soliton Fract 39: 1182-1194. doi: 10.1016/j.chaos.2007.06.004

701   Liberato MLR (2014) The 19 January 2013 windstorm over the North Atlantic: large-scale dynamics and
702   impacts on Iberia. Weather Clim Extremes 5–6: 16–28. doi: 10.1016/j.wace.2014.06.002

703   Linderson M (2001) Objective classification of atmospheric circulation over southern Scandinavia. Int J
704   Climatol 21: 155-169. doi: 10.1002/joc.604

705   Lionello P (2012) The Climate of the Mediterranean Region. From the Past to the Future. Elsevier Insights,
706   London

707   López Lambraño AA (2014) Análisis multifractal y modelación de la precipitación. PhD Thesis, Universidad
708   Autónoma de Querétaro, Querétaro

709   Lovejoy S, Mandelbrot BB (1985) Fractal properties of rain, and a fractal model. Tellus A 37A: 209-232. doi:
710   10.1111/j.1600-0870.1985.tb00423.x

711   Malinverno A (1990) A simple method to estimate the fractal dimension of a self-affine series. Geophys Res
712   Lett 17(11): 1953-1956. doi: 10.1029/GL017i011p01953

713   Mandelbrot BB (1977) The Fractal Geometry of Nature. W H Freeman and Company, New York

714   Martín-Vide J (2002) Aplicación de la clasificación sinóptica automática de Jenkinson y Collison a días de
715   precipitación torrencial en el este de España. In Cuadrat JM, Vicente SM, Saz MA (eds) La información
716   climática como herramienta de gestión ambiental. Universidad de Zaragoza, Zaragoza, pp 123-127

717   Martin-Vide J, Lopez-Bustins JA (2006) The Western Mediterranean Oscillation and rainfall in the Iberian
718   Peninsula. Int J Climatol 26: 1455-1475. doi: 10.1002/joc.1388

719   Martin-Vide J, Sanchez Lorenzo A, Lopez-Bustins JA, Cordobilla MJ, Garcia-Manuel A, Raso JM (2008)
720   Torrential rainfall in northeast of the Iberian Peninsula: synoptic patterns and WeMO influence. Advances in
721   Science and Research 2: 99-105. doi:10.5194/asr-2-99-2008

722   Martín-Vide J (2004) Spatial distribution of a daily precipitation concentration index in Peninsular Spain. Int J
723   Climatol 24: 959-971. doi: 10.1002/joc.1030

724   Meseguer-Ruiz O, Martín-Vide J (2014) Análisis de la fractalidad temporal de la precipitación en Cataluña,
725   España (2010). Investigaciones Geográficas 47: 41-52

726   Meseguer-Ruiz O, Martín-Vide J, Olcina Cantos J, Sarricolea P (2017a) Análisis y comportamiento espacial de
727   la fractalidad temporal de la precipitación en la España peninsular y Baleares (1997-2010). B Asoc Geogr Esp
728   73:11-32. doi: 10.21138/bage.2407

729   Meseguer-Ruiz O, Olcina Cantos J, Sarricolea P, Martín-Vide J (2017b) The temporal fractality of precipitation
730   in mainland Spain and the Balearic Islands and its relation to other precipitation variability indices. Int J
731   Climatol 37(2):849-860. doi: 10.1002/joc.4744

732   Nunes SA, Romani LAS, Avila AMH, Coltri PP, Traina C, Cordeiro RLF, De Sousa EPM, Traina AJM (2013)
733   Analysis of Large Scale Climate Data: How well Climate Change models and data from real sensor networks

734   agree?. In Schwabe D, Almeida V, Glaser H, Baeza-Yates R, Moon S (ed) Proceedings of the IW3C2 WWW
735   2013 Conference, IW3C2 2013, Rio de Janeiro, pp 517-526
736   Oñate Rubalcaba JJ (1997) Fractal Analysis of Climatic Data: Annual Precipitation Records in Spain. Theor
737   Appl Climatol 56: 83-87. doi: 10.1007/BF00863785
738   Osborn TJ, Conway D, Hulme M, Gregory J, Jones PD (1999) Air flow influences on local climate: observed
739   and simulated mean relationships for the United Kingdom. Clim Res 13: 173-191. doi: 10.1006/asle.2000.0013
740   Osborn TJ, Jones PD (2000) Air flow influences on local climate: observed United Kingdom climate variations.
741   Atmos Sci Lett. doi: 10.1006/asle.2000.0017
742   Pérez SP, Sierra EM, Massobrio MJ, Momo FR (2009) Análisis fractal de la precipitación anual en el este de
743   la Provincia de la Pampa, Argentina. Revista de Climatología 9: 25-31
744   Peitgen HO, Jürgens H, Saupe D (1992) Chaos and Fractals: New Frontiers of Science. Springer, New York
745   Pepin NC, Daly C, Lundquist J (2011) The influence of surface versus free air decoupling on temperature trend
746   patterns in the western United States. J Geophys Res 116: D10109. doi:10.1029/2010JD014769
747   Philipp A, Beck C, Huth R, Jacobeit J (2014) Development and comparison of circulation type classifications
748   using the COST 733 dataset and software. Int J Climatol. doi: 10.1002/joc.3920
749   Post P, Truija V, Tuulik J (2002) Circulation weather types and their influence on temperature and precipitation
750   in Estonia. Boreal Environ Res, 7: 281− 289
751   Ramos AM, Trigo RM, Liberato MLR (2016) Ranking of multi-day extreme events over the Iberian Peninsula.
752   Int J Climatol. doi: 10.1002/joc.4726
753   Rasilla Álvarez DF (2003) Aplicación de un método de clasificación sinóptica a la Península Ibérica.
754   Investigaciones Geográficas 30: 27-45
755   Rehman S (2009) Study of Saudi Arabian climatic conditions using Hurst exponent and climatic predictability
756   index. Chaos Soliton Fract 39: 499-509. doi: 10.1016/j.chaos.2007.01.079
757   Rehman S, Siddiqi AH (2009) Wavelet based Hurst exponent and fractal dimensional analysis of Saudi climatic
758   dynamics. Chaos Soliton Fract 40: 1081-1090. doi: 10.1016/j.chaos.2007.08.063
759   Reiser H, Kutiel H (2010) Rainfall uncertainty in the Mediterranean: Intraseasonal rainfall distribution. Theor
760   Appl Climatol 100: 105-121. doi: 10.1007/s00704-009-0162-5
761   Rodríguez R, Casas MC, Redaño A (2013) Multifractal analysis of the rainfall time distribution on the
762   metropolitan area of Barcelona (Spain). Meteorol Atmos Phys 121: 181-187. doi: 10.1007/s00703-013-0256-6
763   Rodríguez-Puebla C, Nieto S (2010) Trends of precipitation over the Iberian Peninsula and the North Atlantic
764   Oscillation under climate change conditions. Int J Climatol 30: 1807-1815. doi: 10.1002/joc.2035
765   Rodríguez-Solà R, Casas-Castillo MC, Navarro X, Redaño Á (2016) A study of the scaling properties of rainfall
766   in Spain and its appropriateness to generate intensity-duration-frequency curves from daily records. Int J
767   Climatol. doi: 10.1002/joc.4738
768   Sáenz J, Zubillaga J, Rodríguez-Puebla C (2001) Interannual variability of winter precipitation in northern
769   Iberian Peninsula. Int J Climatol 21: 1503-1513. doi: 10.1002/joc.699
770   Selvi T, Selvaraj S. 2011. Fractal dimension analysis of Northeast monsoon of Tamil Nadu. Universal Journal
771   of Environmental Research and Technology 1(2): 219-221
772   Sarricolea P, Meseguer-Ruiz O, Martín-Vide J (2014) Variabilidad y tendencias climáticas en Chile central en
773   el período 1950-2010 mediante la determinación de los tipos sinópticos de Jenkinson y Collsion. B Asoc Geogr
774   Esp 64: 227-247
775   Sarricolea P, Meseguer-Ruiz O, Martín-Vide J, Outeiro L (2017) Trends in the frequency of synoptic types in
776   central-southern Chile in the period 1961–2012 using the Jenkinson and Collison synoptic classification. Theor
777   Appl Climatol. doi: 10.1007/s00704-017-2268-5
778   Spellman G (2000) The use of an index-based regression model for precipitation analysis on the Iberian
779   peninsula. Theor Appl Climatol 66: 229-239. doi: 10.1007/s007040070027
780   Spellman G (2016) An assessment of the Jenkinson and Collison synoptic classification to a continental mid-
781   latitude location. Theor Appl Climatol. doi: 10.1007/s00704-015-1711-8
782   Sprott JC (2003) Chaos and Time-Series Analysis. Oxford University Press, Oxford
783   Soriano C, Fernández A, Martin-Vide J (2006) Objective synoptic classification combined with high resolution
784   meteorological models for wind mesoscale studies. Meteorol Atmos Phys 91: 165-181. doi: 10.1007/s00703-
785   005-0133-z
786   Tang L, Chen D, Karlsson PE, Gu Y, Ou T (2009) Synoptic circulation and its influence on spring and summer
787   surface ozone concentrations in southern Sweden. Boreal Environ Res 14: 889-902

788 Trigo R, Dacamara CC (2000) Circulation weather types and their influence on the precipitation regime in
789 Portugal. Int J Climatol 20: 1559-1581. doi: 10.1002/1097-0088(20001115)20:13<1559::AID-
790 JOC555>3.0.CO;2-5
791 Trigo RM, Añel J, Barriopedro D, García-Herrera R, Gimeno L, Nieto R, Castillo R, Allen MR, Massey N
792 (2013) The record winter drought of 2011–12 in the Iberian Peninsula, in explaining extreme events of 2012
793 from a climate perspective. Bull Am Meteorol Soc 94(9): S41–S45
794 Trigo RM, Ramos C, Pereira SS, Ramos AM, Zêzere JL, Liberato MLR (2015) The deadliest storm of the 20th
795 century striking Portugal: Flood impacts and atmospheric circulation. J Hydrol. doi:
796 10.1016/j.jhydrol.2015.10.036
797 Tuček P, Marek L, Paszto V, Janoška Z, Dančák M (2011) Fractal perspectives of GIScience based on the leaf
798 shape analysis. In GeoComputation Conference Proceedings, pp 169-176
799 Veneziano D, Langousis A, Furcolo P (2006) Multifractality and rainfall extremes: A review. Water Resources
800 Research. doi: 10.1029/2005WR004716
801 Vicente-Serrano SM, Trigo RM, Lopez-Moreno JI, Liberato MLR, Lorenzo-Lacruz J, Begueria S, Moran-
802 Tejeda E, El Kenawy A (2011) Extreme winter precipitation in the Iberian Peninsula in 2010: anomalies, driving
803 mechanisms and future projections. Clim Res 46(1): 51–65. doi: 10.3354/cr00977
804 Wolf A, Swift JB, Swinney HL, Vastano JA (1985) Determining Lyapunov exponents from a time series.
805 Physica D 16(3): 285-317. doi: 10.1016/0167-2789(85)90011-9
806 Wolf M (2014) Nearest-neighbor-spacing distribution of prime numbers and quantum chaos. Phys Rev E 89(2):
807 022922, 1-11. doi: 10.1103/PhysRevE.89.022922
808 Zhou X (2004) Fractal and Multifractal Analysis of Runoff Time Series and Stream Networks in Agricultural
809 Watersheds. Virginia Polytechnic Institute and State University, Virginia